

---

This is an electronic reprint of the original article.  
This reprint may differ from the original in pagination and typographic detail.

Pasanen, Toni; Vähänissi, Ville; Theut, Nicholas; Savin, Hele

## Surface passivation of black silicon phosphorus emitters with atomic layer deposited SiO<sub>2</sub>/Al<sub>2</sub>O<sub>3</sub> stacks

*Published in:*

7th International Conference on Silicon Photovoltaics, SiliconPV 2017

*DOI:*

[10.1016/j.egypro.2017.09.304](https://doi.org/10.1016/j.egypro.2017.09.304)

Published: 21/09/2017

*Document Version*

Publisher's PDF, also known as Version of record

*Published under the following license:*

CC BY-NC-ND

*Please cite the original version:*

Pasanen, T., Vähänissi, V., Theut, N., & Savin, H. (2017). Surface passivation of black silicon phosphorus emitters with atomic layer deposited SiO<sub>2</sub>/Al<sub>2</sub>O<sub>3</sub> stacks. In *7th International Conference on Silicon Photovoltaics, SiliconPV 2017* (Vol. 124, pp. 307-312). (Energy Procedia). Elsevier BV.  
<https://doi.org/10.1016/j.egypro.2017.09.304>

---

This material is protected by copyright and other intellectual property rights, and duplication or sale of all or part of any of the repository collections is not permitted, except that material may be duplicated by you for your research use or educational purposes in electronic or print form. You must obtain permission for any other use. Electronic or print copies may not be offered, whether for sale or otherwise to anyone who is not an authorised user.



7th International Conference on Silicon Photovoltaics, SiliconPV 2017

## Surface passivation of black silicon phosphorus emitters with atomic layer deposited SiO<sub>2</sub>/Al<sub>2</sub>O<sub>3</sub> stacks

Toni Pasanen<sup>a,\*</sup>, Ville Vähänissi<sup>a</sup>, Nicholas Theut<sup>b</sup>, Hele Savin<sup>a</sup>

<sup>a</sup>*Aalto University, Department of Electronics and Nanoengineering, Tietotie 3, 02150 Espoo, Finland*

<sup>b</sup>*Arizona State University, Ira A. Fulton Schools of Engineering, Tempe, AZ, United States*

### Abstract

Black silicon (b-Si) is a promising surface structure for solar cells due to its low reflectance and excellent light trapping properties. While atomic layer deposited (ALD) Al<sub>2</sub>O<sub>3</sub> has been shown to passivate efficiently lightly-doped b-Si surfaces and boron emitters, the negative fixed charge characteristic of Al<sub>2</sub>O<sub>3</sub> thin films makes it unfavorable for the passivation of more commonly used n<sup>+</sup> emitters. This work studies the potential of ALD SiO<sub>2</sub>/Al<sub>2</sub>O<sub>3</sub> stacks for the passivation of b-Si phosphorus emitters fabricated by an industrially viable POCl<sub>3</sub> gas phase diffusion process. The stacks have positive charge density ( $Q_{\text{tot}} = 5.5 \cdot 10^{11} \text{ cm}^{-2}$ ) combined with high quality interface ( $D_{\text{it}} = 2.0 \cdot 10^{11} \text{ cm}^{-2} \text{ eV}^{-1}$ ) which is favorable for such heavily-doped n-type surfaces. Indeed, a clear improvement in emitter saturation current density,  $J_{0e}$ , is achieved with the stacks compared to bare Al<sub>2</sub>O<sub>3</sub> in both b-Si and planar emitters. However, although the positive charge density in the case of black silicon is even higher ( $Q_{\text{tot}} = 2.0 \cdot 10^{12} \text{ cm}^{-2}$ ), the measured  $J_{0e}$  is limited by the recombination in the emitter due to heavy doping of the nanostructures. The results thus imply that in order to obtain lower saturation current density on b-Si, careful optimization of the black silicon emitter profile is needed.

© 2017 The Authors. Published by Elsevier Ltd.

Peer review by the scientific conference committee of SiliconPV 2017 under responsibility of PSE AG.

**Keywords:** black silicon; surface passivation; phosphorus diffusion; atomic layer deposition; SiO<sub>2</sub>; Al<sub>2</sub>O<sub>3</sub>

\* Corresponding author. Tel.: +358 50 431 6862.

E-mail address: [toni.pasanen@aalto.fi](mailto:toni.pasanen@aalto.fi)

## 1. Introduction

Black silicon (b-Si) has been of interest of the photovoltaic community already some time due to its excellent light absorption properties. The difficulties in the surface passivation of b-Si have recently been overcome with atomic layer deposited (ALD)  $\text{Al}_2\text{O}_3$  which has been demonstrated both on substrate [1,2] and device level [3,4]. However, there is no proper solution yet presented for the dominating  $\text{n}^+$  emitter as  $\text{Al}_2\text{O}_3$  provides only limited passivation for such emitters due to its negative fixed charge. This problem is enhanced in b-Si since its passivation relies more heavily on the field-effect [5]. Thus, in order to make b-Si a viable option for current PV industry, a conformal thin film with positive fixed charge combined with high quality interface is required.

The negative charge in  $\text{Al}_2\text{O}_3$  has been suggested to originate from electron trapping to O interstitials or Al vacancies as they both produce defect states in the lower half of the band gap and can hence be negatively charged [6]. It has been shown earlier that this negative charge formation in  $\text{Al}_2\text{O}_3$  can be prevented by introducing a thin dielectric layer, e.g. ALD  $\text{SiO}_2$ , between the  $\text{Al}_2\text{O}_3$  thin film and the Si substrate [7]. The  $\text{SiO}_2$  layer acts as an electron tunnel barrier which efficiently prevents charge injection into the trap sites in  $\text{Al}_2\text{O}_3$  [8]. With an interlayer thick enough, the effective total charge density in the  $\text{SiO}_2/\text{Al}_2\text{O}_3$  dielectric stack can be changed to positive due to the fixed and bulk charges in the  $\text{SiO}_2$  film [7].

The potential of ALD  $\text{SiO}_2/\text{Al}_2\text{O}_3$  stacks on the passivation of  $\text{n}^+$  emitters has been studied on planar surfaces by van de Loo *et al.* [9]. With interlayers thicker than 3.6 nm, the authors achieved emitter saturation current densities,  $J_{0e}$ , as low as  $50 \text{ fA/cm}^2$ . Later they applied the stacks also on nanostructured phosphorus emitters and showed that the implied open-circuit voltage ( $i-V_{oc}$ ) was improved from 609 to 640 mV by the introduction of a  $\text{SiO}_2$  interlayer as compared to bare  $\text{Al}_2\text{O}_3$  [10]. However, the reported  $i-V_{oc}$  values were achieved with black silicon that had undergone an alkaline etch treatment to remove sub-surface defects which decreased the height of the silicon needles to only 246 nm and eventually degraded the optical properties of the structure. Moreover, the emitter was made with ion implantation which is not currently a mainstream process in PV industry [11].

This work studies the effectiveness of the positively charged ALD  $\text{SiO}_2/\text{Al}_2\text{O}_3$  dielectric stack for the passivation of b-Si phosphorus emitters fabricated by an industrially feasible  $\text{POCl}_3$  gas phase diffusion process. The optical performance of the deep nanostructures is evaluated after the diffusion and subsequent drive-in process steps to see how well the structures withstand these processes. Additionally, the film properties are characterized by interface defect density,  $D_{it}$ , charge density,  $Q_{tot}$  and emitter saturation current density,  $J_{0e}$ .

## 2. Experimental details

Black silicon was etched on both sides of p-type CZ wafers ( $20 \text{ }\Omega\text{cm}$ ,  $675 \text{ }\mu\text{m}$ ) by deep reactive ion etching using process parameters reported in [12]. Emitters were formed in a tube furnace by  $\text{POCl}_3$  diffusion at two different temperatures: 830 and 800 °C ( $\text{POCL}_{830}$  and  $\text{POCL}_{800}$ , respectively).  $\text{POCl}_3$  gas was introduced for 20 minutes, followed by a 5 min drive-in in an  $\text{O}_2$  ambient at the same temperature. Sheet resistance was measured with four-point probe and confirmed later by an inductive coupling based method. The higher diffusion temperature resulted in sheet resistances of 95 and 53  $\Omega/\square$  and the lower temperature in 225 and 113  $\Omega/\square$  in planar and b-Si samples, respectively. Profiles of total and electrically active phosphorus concentration were measured from planar samples with secondary ion mass spectrometry (SIMS) and electrochemical capacitance-voltage (ECV) profiling method, respectively. Profiles in b-Si were not measured due to instrumental limitations to measure doping concentration accurately in the case of nanostructured surfaces.

After the phosphosilicate glass (PSG) removal in 5% HF, the samples were passivated with either 22 nm of ALD  $\text{Al}_2\text{O}_3$  or a stack of 6.5 nm of plasma-enhanced ALD  $\text{SiO}_2$  and 30 nm of thermal ALD  $\text{Al}_2\text{O}_3$ . A commercial Si precursor and  $\text{O}_2$  plasma were used for  $\text{SiO}_2$ , whereas TMA +  $\text{H}_2\text{O}$  process was utilized for  $\text{Al}_2\text{O}_3$ . All depositions were performed at 200 °C. The passivation was subsequently activated by annealing the samples at 400 °C for 30 min in  $\text{N}_2$  ambient. The conformality of the ALD films on high aspect ratio nanostructures was confirmed with scanning electron microscopy (SEM, Fig. 1a).

To characterize the passivation quality, emitter saturation current density,  $J_{0e}$ , was extracted from the measured quasi-steady-state photoconductance (QSSPC) lifetime data at an injection level of  $10^{16} \text{ cm}^{-3}$ . In the extraction, Auger model according to Richter *et al.* was applied which takes the band gap narrowing into account [13,14]. In

addition, to study the passivation properties more thoroughly, total oxide charge density,  $Q_{\text{tot}}$ , and interface defect density,  $D_{\text{it}}$ , were determined from separate lifetime samples processed in the same ALD runs by contactless CV (COCOS) method [15]. Finally, positive corona charge was deposited onto the samples to study the effect of surface charge on the passivation and the resulting  $J_{0c}$ . The actual amount of deposited charge was determined by measuring the change in the contact potential difference between a Kelvin probe and the silicon substrate in every deposition step.

### 3. Results and discussion

Doping profiles measured from the planar reference samples are presented in Fig. 1b. The difference between the total and electrically active phosphorus concentration measured with SIMS and ECV, respectively, in the POCL\_830 profiles near the sample surface indicates the presence of inactive dopants. Moreover, based on the sheet resistance values shown as an inset in Fig. 1b, the enhanced surface area of b-Si results in a larger amount of phosphorus in those emitters. As the silicon needles are covered with phosphosilicate glass on all sides, more phosphorus diffuses into the substrate during the drive-in. Similar observations have also been reported earlier [16, 17]. In this study, the sheet resistance in the nanostructured samples is found to be 1.8–2 times that in the planar counterparts. Thus, a considerably higher amount of phosphorus in the b-Si samples is expected, which indicates that emitter recombination will most likely be limiting the  $J_{0c}$ .

Possible effect of the diffusion and thin film deposition processes on the optical properties of b-Si is evaluated by surface reflectance measurements. The reflectance of a b-Si surface after  $\text{POCl}_3$  diffusion and PSG removal as a function of wavelength, shown in Fig. 1c, proves that the structure retains its excellent optical properties in the diffusion process despite the oxidizing drive-in step. Indeed, the reflectance remains below 1 % for almost the whole sun spectrum range. This observation hence promises that diffusion parameters can be tailored to optimize the emitter profile without significant tradeoffs in the low reflectance of black silicon. The deposition of a  $\text{SiO}_2/\text{Al}_2\text{O}_3$  stack slightly increases the reflectance in the wavelength range of 400–1000 nm but enhances the optical properties in the UV region. This change is caused by the interference of light rays reflected from the interfaces of the dual-layer structure and the substrate. The two materials in the stack with refractive indices of 1.47 and 1.62 for ALD  $\text{SiO}_2$  and  $\text{Al}_2\text{O}_3$ , respectively, reduce surface reflectance especially in the short wavelength range with the selected film thicknesses, which can be observed also from the relatively low reflectance of the planar reference sample in the UV region. This improvement in combination with the optical properties of b-Si results in the observed flat spectral reflectance in the wavelength range of 300–1000 nm. This low reflectance corresponds to  $\sim 98$  % absorbance.

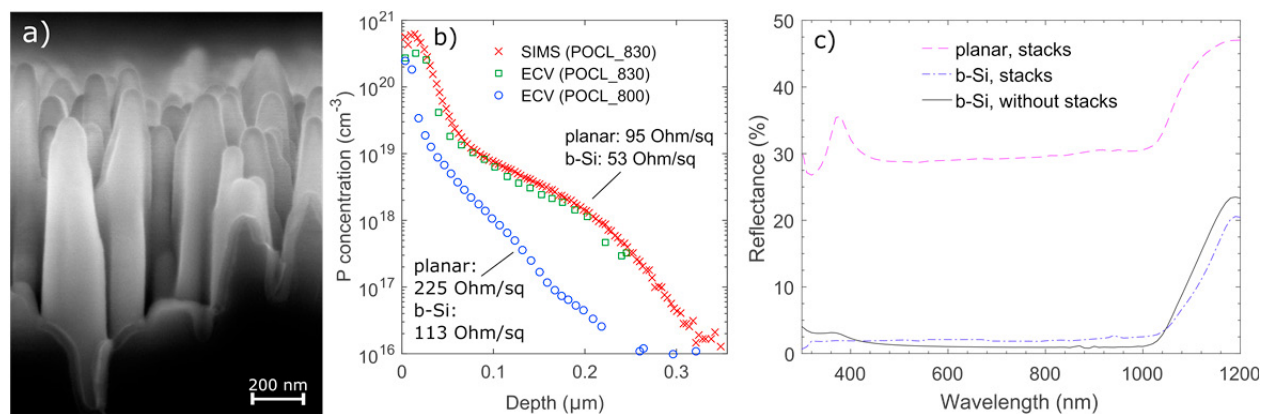


Fig. 1. a) SEM image of b-Si conformally covered with 6.5 nm of ALD  $\text{SiO}_2$  + 30 nm of  $\text{Al}_2\text{O}_3$ . b) Doping profiles of two planar samples measured with ECV. In addition, a SIMS profile of a POCL\_830 diffused sample is presented. The measured sheet resistance values are shown as an inset, including b-Si samples. c) Reflectance of a nanostructured surface after  $\text{POCl}_3$  diffusion and PSG removal (black solid line), and after subsequent deposition of the stacks. As a reference, reflectance of a planar surface covered with the stacks is shown.

Fig. 2a presents emitter saturation current densities for both planar and b-Si samples with two different emitter profiles, POCL\_830 and POCL\_800, and two different ALD passivation schemes, bare  $\text{Al}_2\text{O}_3$  and  $\text{SiO}_2/\text{Al}_2\text{O}_3$  stacks. As hypothesized, the  $\text{SiO}_2/\text{Al}_2\text{O}_3$  stacks provide lower  $J_{0e}$  values compared to bare  $\text{Al}_2\text{O}_3$  in all cases due to the more suitable polarity of the oxide charge (Fig. 2b). Although the absolute value of  $Q_{\text{tot}}$  is lower in the oxide stack, it outperforms the negatively charged  $\text{Al}_2\text{O}_3$  in  $J_{0e}$  since the doping concentration in the emitter is too high for the negative charges in  $\text{Al}_2\text{O}_3$  to induce inversion. In addition, approximately three times higher effective charge density was measured from b-Si samples compared to the planar references, which is in agreement with the previously reported results [5]. Better passivation provided by the  $\text{SiO}_2/\text{Al}_2\text{O}_3$  stacks can partly be explained also by the lower mid-gap interface defect density, as presented in Fig. 2b. This reduction in  $D_{\text{it}}$  is caused by hydrogen diffusion from the  $\text{Al}_2\text{O}_3$  film to the Si/SiO<sub>2</sub> interface during post-deposition annealing [18]. Mid-gap  $D_{\text{it}}$  is reported only for the planar samples since its extraction from COCOS measurements in the case of b-Si is not yet unambiguously defined. The improvement in  $J_{0e}$  is higher in the samples with lower doping concentration (*i.e.*, POCL\_800) which can be attributed to a smaller amount of inactive phosphorus and less dominating Auger recombination.

The surface passivation quality, as characterized by  $D_{\text{it}}$  and  $Q_{\text{tot}}$  (Fig. 2b), indicated better  $J_{0e}$  values than were measured in the stacked samples. In order to study whether the reason for the rather high  $J_{0e}$  values was due to insufficient level of field-effect passivation or emitter recombination, positive corona charge was deposited onto the samples. As shown in Fig. 3,  $J_{0e}$  of the  $\text{Al}_2\text{O}_3$  passivated samples, both planar and b-Si, was reduced substantially by the deposition of positive charge, as expected and previously reported in literature [9]. On the contrary, positive corona charge had barely any impact on the samples passivated with the stacks. Furthermore,  $J_{0e}$  saturated to approximately same value for both  $\text{Al}_2\text{O}_3$  and  $\text{SiO}_2/\text{Al}_2\text{O}_3$  passivated planar samples. Thus, this value can be considered as the  $J_{0e}$  limited by Auger and Shockley-Read-Hall (SRH) recombination in the emitter region, the latter caused by defect states introduced by inactive phosphorus [19]. Therefore, lower values could be achieved only by designing the emitter profiles further in order to avoid excessive doping. Similar trends are observed with both POCL\_830 and POCL\_800 diffusion profiles, the effect of corona charge being more significant in the samples with less doping (*i.e.*, POCL\_800) due to less dominating Auger recombination and a smaller amount of inactive phosphorus. The same reason also explains the steeper decrease in the  $J_{0e}$  of the planar samples as the b-Si counterparts have higher doping concentration.

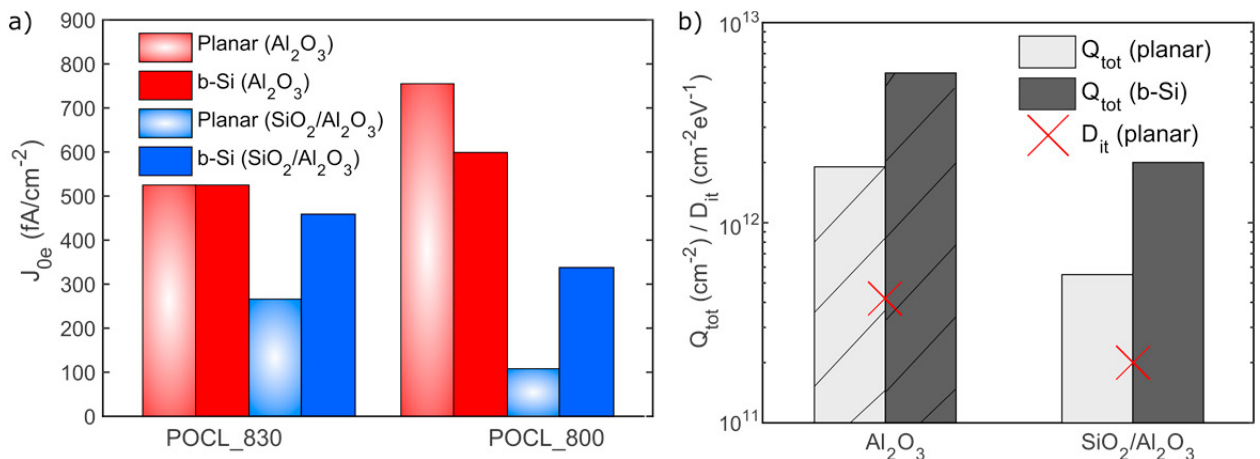


Fig. 2. a) Emitter saturation current density of phosphorus emitter samples passivated with either  $\text{SiO}_2/\text{Al}_2\text{O}_3$  stacks or bare  $\text{Al}_2\text{O}_3$ . b) Total charge and interface defect density after annealing of the dielectric layers obtained with the COCOS method. The values are extracted from separate lifetime samples processed in the same ALD runs with the emitters. The charge of bare  $\text{Al}_2\text{O}_3$  is negative as indicated by the diagonal stripes.  $D_{\text{it}}$  values are determined from the planar samples.

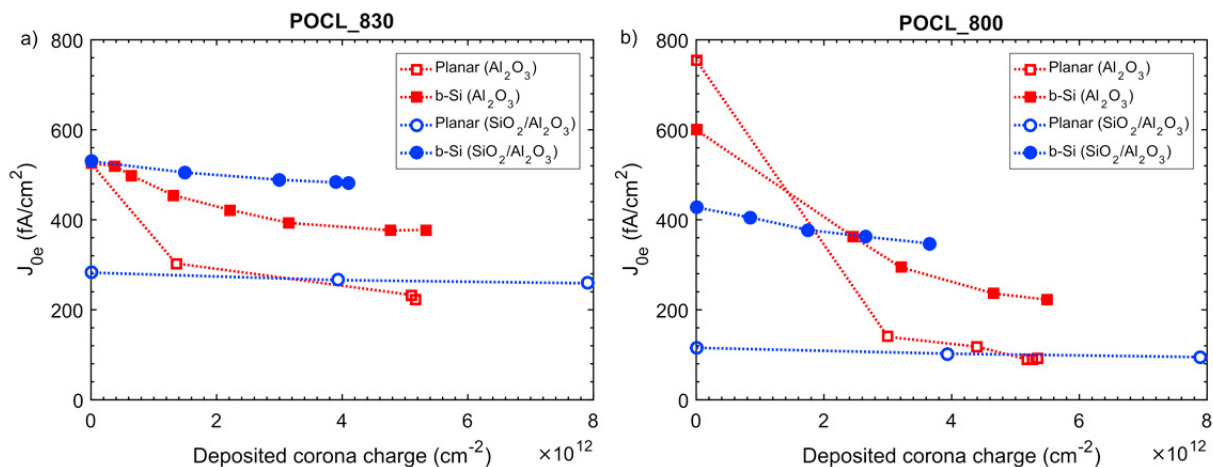


Fig. 3.  $J_{0e}$  as a function of deposited corona charge density for two different emitter profiles: a) POCL\_830 and b) POCL\_800. Open symbols denote planar and filled symbols b-Si samples. The deposited charge reduces the  $J_{0e}$  of the  $\text{Al}_2\text{O}_3$  passivated samples considerably, while it has barely any impact on the  $\text{SiO}_2/\text{Al}_2\text{O}_3$  passivated samples. In the samples with lighter doping (*i.e.*, POCL\_800), the effect is more significant. The  $J_{0e}$  limited by Auger and SRH recombination caused by inactive phosphorus is higher in the b-Si samples.

In the case of b-Si samples, however, somewhat lower  $J_{0e}$  values were obtained with bare  $\text{Al}_2\text{O}_3$  than with the stacks by corona charging, as visible in Fig. 3a-b. This could be explained by weaker chemical passivation provided by the stacks on b-Si, opposite to what observed from the planar samples by COCOS method. However, the interface quality in the case of b-Si cannot be directly concluded from the  $D_{it}$  values measured from the corresponding planar samples. For instance, rather short ALD precursor pulse and purge steps may provide excellent thin film quality on planar surfaces, but result in an imperfect film on b-Si due to the high aspect ratio of the nanotexture [20]. Thus, the corona charging experiments indicate that the full potential of the  $\text{SiO}_2/\text{Al}_2\text{O}_3$  stacks was not reached on b-Si, but even larger improvement in  $J_{0e}$  could be achieved by fine tuning the ALD process parameters for nanostructured surfaces.

The  $J_{0e}$  values measured from the planar samples passivated with the stacks are comparable to results reported by Bordihn *et al.* where the  $\text{SiO}_2$  interlayers were deposited by PECVD [21]. The authors achieved a  $J_{0e}$  of  $\sim 200$  fA/cm<sup>2</sup> in an  $n^+$  emitter with a doping profile close to that of POCL\_830. Thus, the electrical properties of  $\text{SiO}_2/\text{Al}_2\text{O}_3$  stacks are not limited to ALD films only, although for b-Si, this deposition method is most likely the only viable option due to the high aspect ratio of the nanostructures. Although direct comparison with results on implanted b-Si emitters is challenging, the performance of the stacks on phosphorus-diffused b-Si emitters is consistent with the implied  $V_{oc}$  of 616–640 mV reported by van de Loo [10], the corresponding values being 626 mV and 633 mV in the samples with POCL\_830 and POCL\_800 profiles, respectively.

#### 4. Conclusions

This work studied the potential of ALD  $\text{SiO}_2/\text{Al}_2\text{O}_3$  stacks for b-Si  $n^+$  emitter passivation. The positive fixed charge in the stacks resulted in lower emitter saturation current densities compared to bare  $\text{Al}_2\text{O}_3$  which is a promising step towards the implementation of b-Si in commercial p-type silicon solar cells. However, the  $J_{0e}$  values in b-Si were in general higher than the corresponding planar references, mainly due to recombination in the heavily doped emitter that was not optimized for b-Si. Black silicon emitters suffered from enhanced excessive doping and a large amount of inactive phosphorus resulting in large Auger and SRH recombination which was found by corona charging. These experiments also revealed that the full potential of the stacks was not reached on b-Si, but even higher improvement in  $J_{0e}$  could be achieved by fine tuning the diffusion and ALD process parameters for nanostructured surfaces.

## Acknowledgements

The authors acknowledge the provision of facilities by Aalto University at OtaNano - Micronova Nanofabrication Centre. This work was funded by the BLACK project (project No. 2956/31/2014) which is supported under the umbrella of SOLAR-ERA.NET by the Finnish Funding Agency for Innovation TEKES. The authors thank Sebastian Husein and Tara Nietzold for performing the ECV measurements. Hannu Laine is acknowledged for helpful discussions.

## References

- [1] Repo P, Haarahiltunen A, Yli-Koski M, Talvitie H, Sainiemi L, Schubert MC, Savin H. Passivation of black silicon surfaces with ALD  $\text{Al}_2\text{O}_3$  in 2nd International Conference on Silicon Photovoltaics, SiliconPV, Leuven, Belgium, 2012.
- [2] Otto M, Kroll M, Käsebier T, Salzer R, Tünnermann A, Wehrspohn RB. Extremely low surface recombination velocities in black silicon passivated by atomic layer deposition. *Applied Physics Letters* 2012;100:191603.
- [3] Savin H, Repo P, von Gastrow G, Ortega P, Calle E, Garin M, Alcubilla R. Black silicon solar cells with interdigitated back-contacts achieve 22.1% efficiency. *Nature Nanotechnology* 2015;10:624-628.
- [4] Juntunen MA, Heinonen J, Vähänissi V, Repo P, Valluru D, Savin H. Near-unity quantum efficiency of broadband black silicon photodiodes with an induced junction. *Nature Photonics* 2016;10:777-781.
- [5] von Gastrow G, Alcubilla R, Ortega P, Yli-Koski M, Conesa-Boj S, Fontcuberta i Morral A, Savin H. Analysis of the atomic layer deposited  $\text{Al}_2\text{O}_3$  field-effect passivation in black silicon. *Solar Energy Materials & Solar Cells* 2015;142:29-33.
- [6] Weber JR, Janotti A, van de Walle CG. Native defects in  $\text{Al}_2\text{O}_3$  and their impact on III-V/ $\text{Al}_2\text{O}_3$  metal-oxide-semiconductor-based devices. *Journal of Applied Physics* 2011;109:033715.
- [7] Dingemans G, Terlinden NM, Verheijen MA, van de Sanden MCM, Kessels WMM. Controlling the fixed charge and passivation properties of  $\text{Si}(100)/\text{Al}_2\text{O}_3$  interfaces using ultrathin  $\text{SiO}_2$  interlayers synthesized by atomic layer deposition. *Journal of Applied Physics* 2011;110:093715.
- [8] Terlinden NM, Dingemans G, Vandalon V, Bosch RHEC, Kessels WMM. Influence of the  $\text{SiO}_2$  interlayer thickness on the density and polarity of charges in  $\text{Si}/\text{SiO}_2/\text{Al}_2\text{O}_3$  stacks as studied by optical second-harmonic generation. *Journal of Applied Physics* 2014;115:033708.
- [9] van de Loo BHW, Knoops HCM, Dingemans G, Janssen GJM, Lamers MWPE, Romijn IG, Weeber AW, Kessels WMM. "Zero-charge"  $\text{SiO}_2/\text{Al}_2\text{O}_3$  stacks for the simultaneous passivation of  $\text{n}^+$  and  $\text{p}^+$  doped silicon surfaces by atomic layer deposition. *Solar Energy Materials & Solar Cells* 2015;143:450-456.
- [10] van de Loo B, Ingenito A, Isabella O, Zeman M, Verheijen M, Kessels E. ALD  $\text{SiO}_2/\text{Al}_2\text{O}_3$  stacks for the passivation of phosphorus-doped black-Si surfaces in 6th International Conference on Silicon Photovoltaics, SiliconPV, Chambéry, France, 2016.
- [11] International Technology Roadmap for Photovoltaic Results 2016. 8th Edition, 2017.
- [12] Repo P, Haarahiltunen A, Sainiemi L, Yli-Koski M, Talvitie H, Schubert M, Savin H. Effective passivation of black silicon surfaces by atomic layer deposition. *IEEE Journal of Photovoltaics* 2013;3:90-94.
- [13] Richter A, Glunz SW, Werner F, Schmidt J, Cuevas A. Improved quantitative description of Auger recombination in crystalline silicon. *Physical review B* 2012;86:165202.
- [14] Kimmerle A, Rothhardt P, Wolf A, Sinton RA. Increased reliability for  $J_0$ -analysis by QSSPC. *Energy Procedia* 2014;55:101-106.
- [15] Wilson M, Lagowski J, Jastrzebski L, Savtchouk A, Faifer V. COCOS (corona oxide characterization of semiconductor) non-contact metrology for gate dielectrics. *AIP Conference Proceedings* 2001;220-225.
- [16] Oh J, Yang HC, Branz HM. An 18.2%-efficient black-silicon solar cell achieved through control of carrier recombination in nanostructures. *Nature Nanotechnology* 2012;7:743-748.
- [17] Kafle B, Schön J, Fleischmann C, Werner S, Wolf A, Clochard L, Duffy E, Hofmann M, Rentsch J. On the emitter formation in nanotextured silicon solar cells to achieve improved electrical performances. *Solar Energy Materials & Solar Cells* 2016;152:94-102.
- [18] Dingemans G, Beyer W, van de Sanden MCM, Kessels WMM. Hydrogen induced passivation of Si interfaces by  $\text{Al}_2\text{O}_3$  films and  $\text{SiO}_2/\text{Al}_2\text{O}_3$  stacks. *Applied Physics Letters* 2010;97:152106.
- [19] Min B, Wagner H, Dastgheib-Shirazi A, Altermatt PP. Limitation of industrial phosphorus-diffused emitters by SRH recombination. *Energy Procedia* 2014;55:115-120.
- [20] Elam JW, Routkevitch D, Mardilovich PP, George SM. Conformal coating on ultrahigh-aspect-ratio nanopores of anodic alumina by atomic layer deposition. *Chemistry of Materials* 2003;15:3507-3517.
- [21] Bordihn S, Dingemans G, Mertens V, Müller JW, Kessels WMM. Passivation of  $\text{n}^+$ -type Si surfaces by low temperature processed  $\text{SiO}_2/\text{Al}_2\text{O}_3$  stacks. *IEEE Journal of Photovoltaics* 2013;3:925-929.